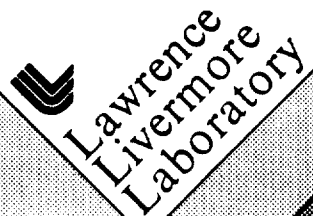UCRL- *85016*
PREPRINT

Energy Flow in High Speed Perforation and Cutting

M. van Thiel

This paper was prepared for submittal to
31st Aeroballistic Range Assn. Conference
Pasadena, CA

October 7, 1980

Lawrence Livermore Laboratory

DISCLAIMER

ENERGY FLOW IN HIGH SPEED PERFORATION AND CUTTING*

M. van Thiel

ABSTRACT

It is demonstrated that effects of long rod penetrators on targets can be modeled by introducing a high pressure (energy) column on the penetration path in place of the projectile. This energy can be obtained from the kinetic energy of the penetrator; the equations of state of the materials used and a Bernoulli penetration condition. The model is supported by detailed hydro calculations.

INTRODUCTION

Two-stage guns are capable of yielding the information needed to describe the effects of high, if not hypervelocity impacts. Perez[1] has given data for 5 km/s impact velocity while Christman[2] went to 6.7 km/s. Using smaller rods, the same gun used by Christman is capable of velocities approaching 8 km/s. Fig. 1 is a calculated rod target interaction that indicates the complexity of the detailed problem. A computer code like the one used here is capable of computing the details of the wave interactions and surface acceleration.

The initial impact pressure is higher than the steady state penetration pressure. For flat-nosed or blunt projectiles it is equivalent to a 1-D impact pressure. This pressure wave spreads and decays as the interface pressure is also decreases to the steady state Bernoulli condition. As the stresswave travels through the target its pressure tends to be reduced by the free surfaces, while at the same time it is fed by the energy of the penetrator. The problem is too complex to allow a detailed understanding and the hydrocalculations are time consuming. But experiments and simple models can yield further physical insights, that can then be applied to practical problems. Such a simple modeling approach is described here.

THEORY

The problem presented here will address the amount of surface motion produced by a long rod projectile moving at 8 km/s. We will use a simple model which we shall call the Prompt Energy Deposition model because we imagine the energy of the jet to be deposited instantaneously and then transmitted to the surfaces.

Fig. 2 is a case of a plate penetrating a plate - a 2-D calculation. The energy source for the surface motion is a sheet of high pressure material with the thickness of the penetrator that also has the proper kinetic energy. That energy and momentum may be generated by considering an equivalent, one-dimensional process. Each element of the high energy sheet acts independently on each element of the target surface, the total effect is the integral over the high energy zone. We note as shown in Fig. 2, that the integral of the surface kinetic energy is equivalent to the integral over the same surface of the energy deposited in each surface element. That energy is proportional to the energy in each element of the high pressure zone modified by an attenuation function $f(r)$ and constant K, where r is the distance between the elements. This approach allows scaling between different impactor energies and immediately leads to the result for a rod with proper consideration for the differences in geometry. Note that for any surface element B, r is a function of h while (per unit width) $dA = dr'$.

The key for the success of this procedure is the proper method for determining the energy density (E) and the attenuation function f(r). The interface velocity between impactor and target can be readily computed with three different flow paths. <u>A</u> a Bernoulli flowpath, <u>B</u> a shockwave path, and <u>C</u> an isentropic one-dimensional compression path. All these processes achieve the same velocity within a percent or two. The two 1-D processes. B and C also achieve the same interface pressure while the Bernoulli flow process yields a lower value. The principal difference is that in the Bernoulli flow process the flow is not constrained to one dimension. Nevertheless, the initial decrease in the kinetic energy of the projectile is the same. The difference is due to lateral flow which decreases the potential energy density and increases the amount of materials under pressure. We therefore postulate that we can select a 1-D compression path to determine the potential energy deposited in the target.

The next question deals with the material in the high energy column. We are dealing with both projectile and target material in some proportion. We determine this ratio using the incompressible Bernoulli penetration condition,

$$\frac{h}{\cos\theta} = \text{Pen} = \int U.dt = \ell \cdot \frac{U}{V-U} = \ell \cdot \left[\rho_{0p}/\rho_{0t}\right]^{1/2}$$

to determine the length of projectile used up in the process. Since the projectile is compressed in the 1-D process selected the fraction of projectile material is

$$\alpha = \left[\rho_{0t}/\rho_{0p}\right]^{1/2} \left[\rho_{0p}/\rho_p{}^{(P)}\right] \cdot$$

This proportion may then be used in the determination of the equation of state of the mixture from the equations of state of the two materials.

RESULTS

The data base for the verification of the model was obtained from a coupled Eulerian-Lagrange calculation. The hydrocode is called CHAMP[2] (for A Coupled HEMP[4] Multifluid Eulerian[5] Program for Fluid Flow Simulations) and was produced at LLNL. The Eulerian part of the code allows minimum pressure and density cutoffs for the pressure calculation which describes some of the effects of spall or vaporization. The Lagrange part is fully elastic-plastic with a spall criterion. Neither spall nor vaporization were significant in the Eulerian part of the grid and spall played a minor role in the motion of the Lagrange grid. Figs. 3 and 4 show the material boundaries in the Eulerian portion and the grid of the Lagrange section. The zone size in the Eulerian section is about half as large as the small Lagrange zones. The qualitative features of the plate-plate penetration are similar to the rod-plate case. The most easily noticeable difference is the rate of void growth, which is larger in the plate-plate case, otherwise the configurations look alike.

The model-hydro correlation in Fig. 5 is good. First of all, a simple exponential fits the motion of the exit surface in the plate-plate penetration calculation. The required geometric changes to describe the rod-plate pentration produce the dashed curve. While the fit is still reasonably good, a definite deviation is observable. At a small distance from the rod exit point, the model underestimates the kinetic energy of the surface while at large distrances the opposite is true.

A related difference between plate and rod penetrator processes is the lateral (radial) momentum change. While the lateral velocity of the plate that is cut by a plate is always positive (away from the cut), this is not true if the plate is perforated with a rod. Fig. 6 shows the radial surface velocity profile at two different times. At 17 microseconds we see the remnant of an elastic precursor and a deformational wave following it. Behind this wave the velocity decreases and then increases again as the distance from the penetration point decreases. Later in time, the motion beyond 45 mm has reversed itself and some of the material is contracting back toward the hole.

This elastic reverberation is of course absent in the cut plate, since no restoring forces exist here. The unique difference therefore lies in the hoop stress. The effect of tensile forces is also noticeable on the impact surface of the plate. The momentum transferred to the plate introduces a direction to the motion, while the potential energy term produced by the pressure is nondirectional. The integral for the velocity of a surface element is therefore

$$0.5\rho v^2 (Y) = K \frac{\pi n_D^{n+1}}{2^{2n}(\cos\theta)^{n+1}} \int^h (\phi + 0.5\rho_0 U_B^2 \frac{\cos^3\alpha}{(\cos\alpha)} \frac{e^{-\beta r}}{\ell^n} \, dh \quad .$$

Here n is 0 for the plate-plate and 1 for the rod-plate case, $\phi = \int_{V0} P dV$ is the potential energy and U_B is the Bernoulli interface velocity. The two terms in brackets subtract on the impact surface (for small θ) and the kinetic term dominates close to the point of entry.

The result of this formulation is shown in Fig. 7. Here we note that the velocities on the exit surface are larger than on the impact surface. The potential energy term alone, overestimates the deposited energy. The kinetic term appears to yield the proper adjustment until we reach a region where tension forces become large. At that point, the kinetic term clearly does not couple into the surface motion due to yield and spall effects.

CONCLUSION

We have shown that a simple energy attenuation function may be used to approximate the energy deposited on the surface of a plate penetrated by a rod or a plate. Deviations from the simple model can be related to strength effects.

REFERENCES

1. E. Perez, "A Theory for Armor Penetration by Hypervelocity Long Rods",
    Fourth Int. Symp. on Ballistics (American Defense Preparedness Assn.
    1978).

2. D. R. Christman and J. W. Gehring, J. Appl. Phys. 37, 1579 (1966).

3. L. L. Edwards, R. B. Heckman, J. K. Hobson and T. C. Michels, "CHAMP: A
    Coupled HEMP and Multifluid Eulerian Program for Fluid Flow Simulations".
    (LLNL Lab. Report UCRL 52444, 1978).

4. M. L. Wilkins "Calculations of Elastic-Plastic Flow" (LLNL Lab. Report
    UCRL-7322, Rev. 1, 1969).

5. W. F. Noh, "CEL: A Time-Dependent, Two-Space-Dimensional, Coupled
    Eulerian-Lagrange Code," Methods in Computational Physics, B. Alder,
    S. Fernback and M. Rotenberg, Eds. (Academic Press, NY 1964) Vol. 3,
    p. 117.

FIGURE CAPTIONS

1. Detailed hydrocalculation of a high velocity long rod penetration. Lagrange grid of the iron target and Eulerian boundaries of penetrator (Ni) and target (Fc).

2. Schematic presenttion of the significant parameters in the Prompt Energy deposition model and energy balance equation for the surface kinetic energy.

3. Lagrange grid and Eulerian material boundaries at + = 0.

4. Lagrange grid and Eulerian materal boundaries at + = 8.5 us.

5. Model fit of the kinetic energy at the target exit surface for: a plate-plate penetration (+ hydrocalculation, _____ model calculation), and b the rod-plate penetration (. hydrocalcualtion, - - - model calculation.)

6. Radial velocity versus radius on the exit surface of the target at t = 1 and t = 22 us.

7. Surface velocities for the plate-plate penetration case: _____ model exit-surface-velocity-squared; _____ model impact surface velocity squared; x hydro result for the impact surface.
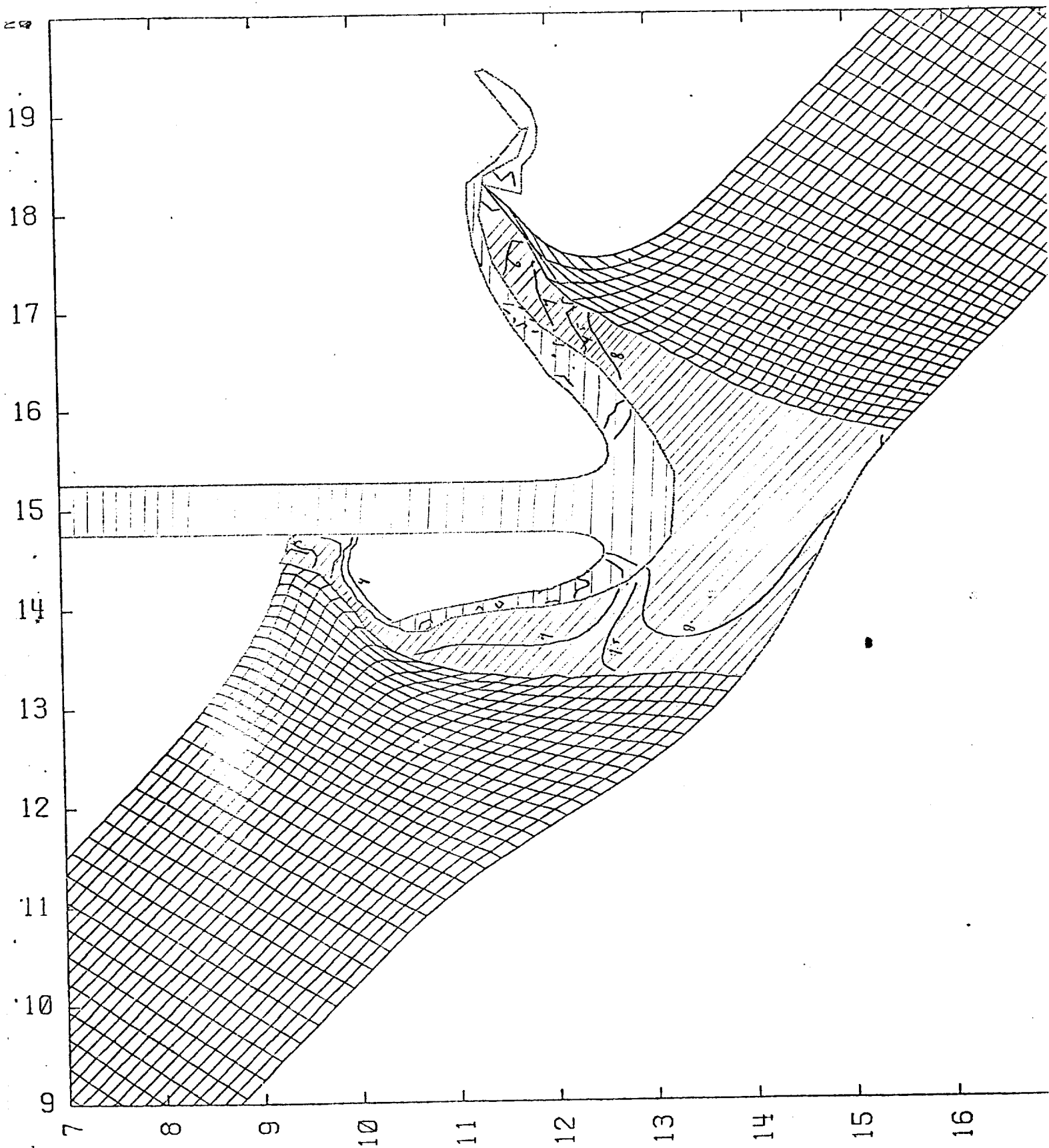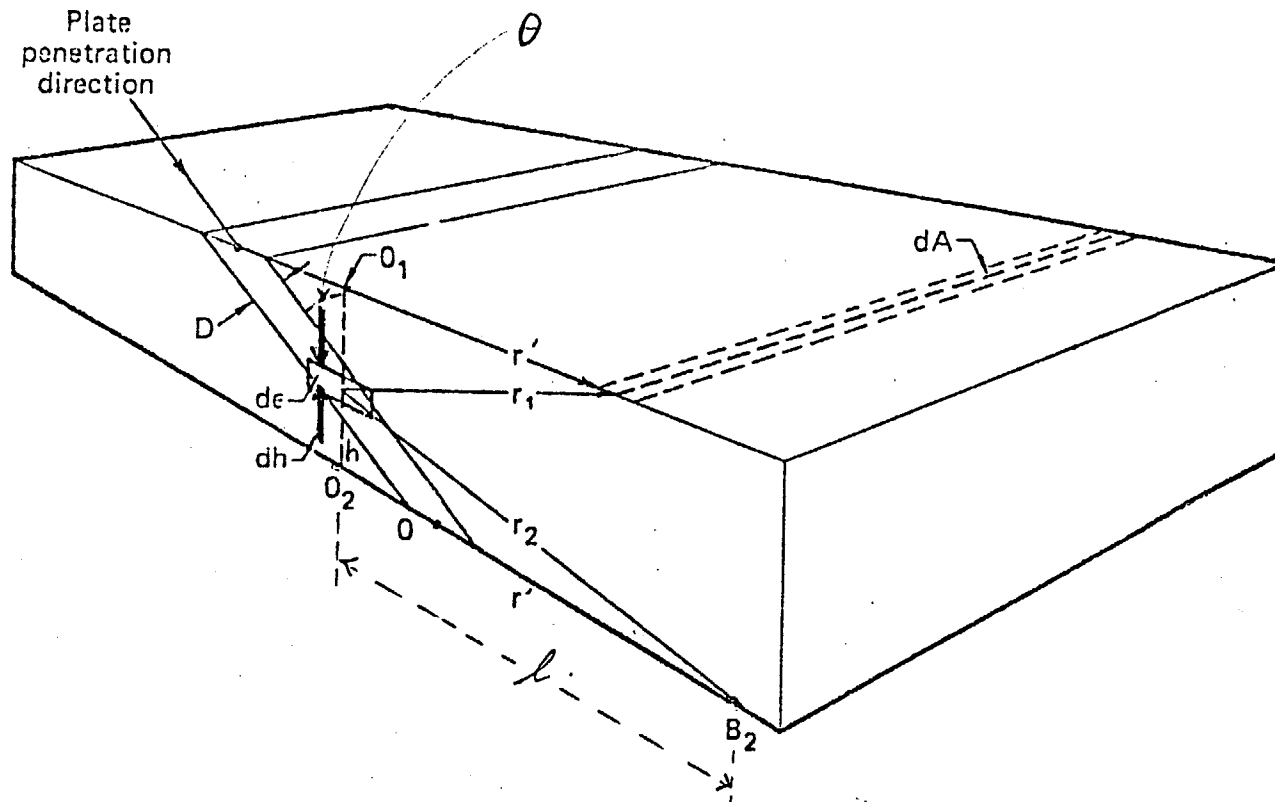
Fig. 1

PROMPT ENERGY DEPOSITION MODEL

$$\int_t^A .5 \rho \, \mathcal{V}^2 \, dA = K \int^{r'} dr' \int^h \frac{\in D}{\cos\theta} \; f(r_2) \; dh$$

Fig. 2

ISORHO
A 2.00E+00
B 5.00E+00
C 7.80E+00
D 8.50E+00
E 9.00E+00

1.00E+01

9.00E+00

8.00E+00

7.00E+00

6.00E+00

5.00E+00

4.00E+00

3.00E+00

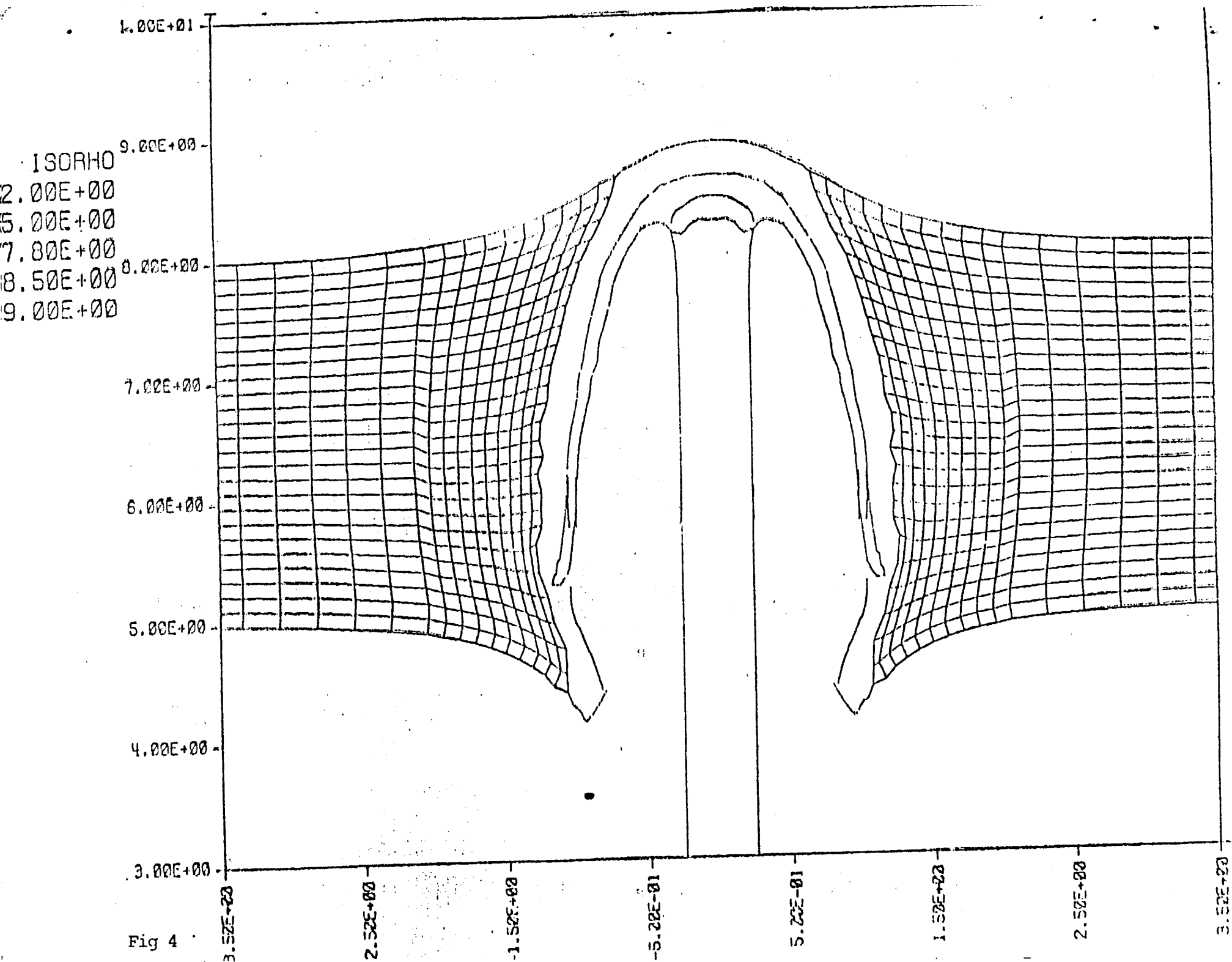3.50E+00 2.50E+00 1.50E+00 5.00E-01 5.00E-01 1.50E+00 2.50E+00 3.50E+00

Fig 3

ISORHO
2.00E+00
5.00E+00
7.80E+00
8.50E+00
9.00E+00

Fig 4
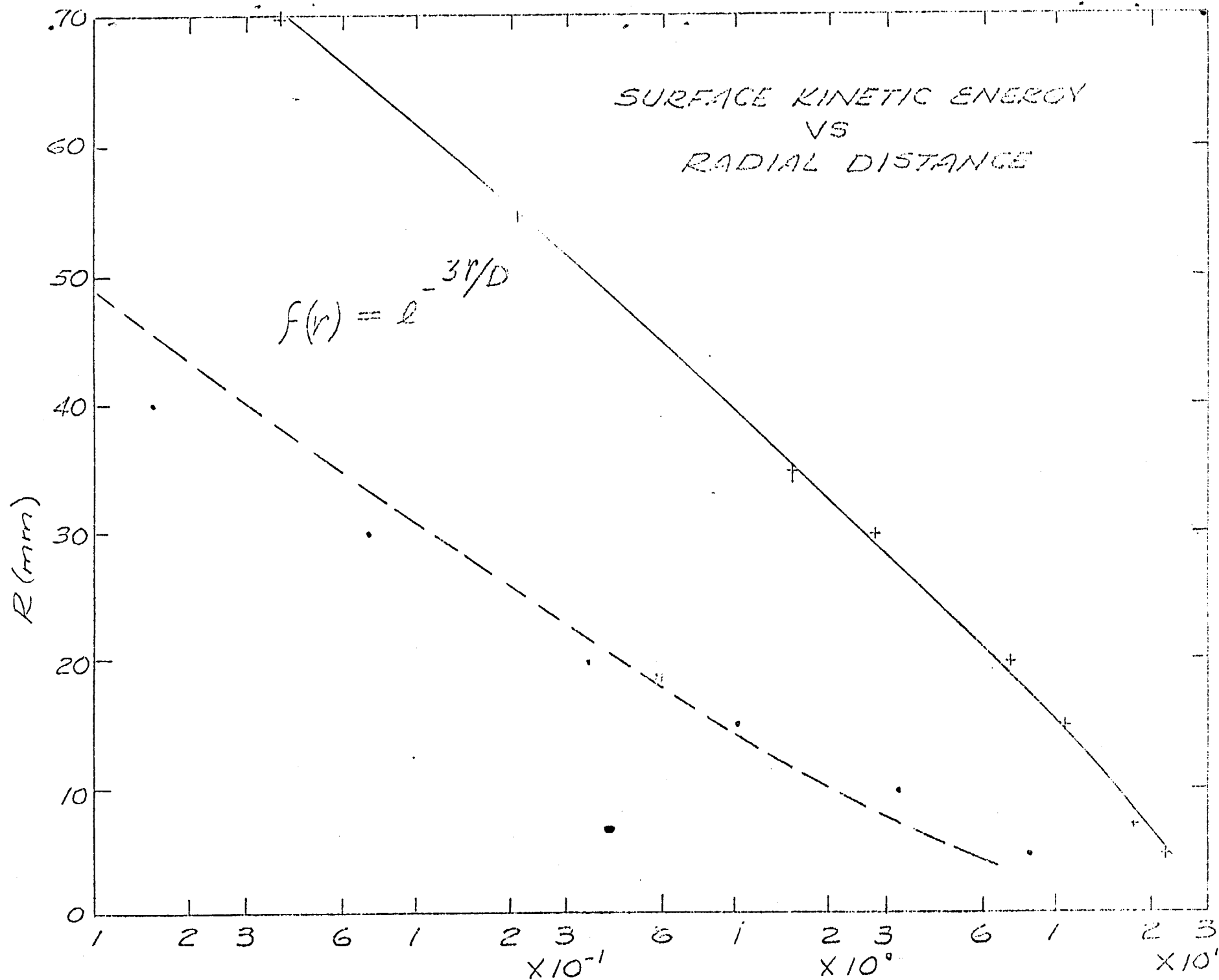
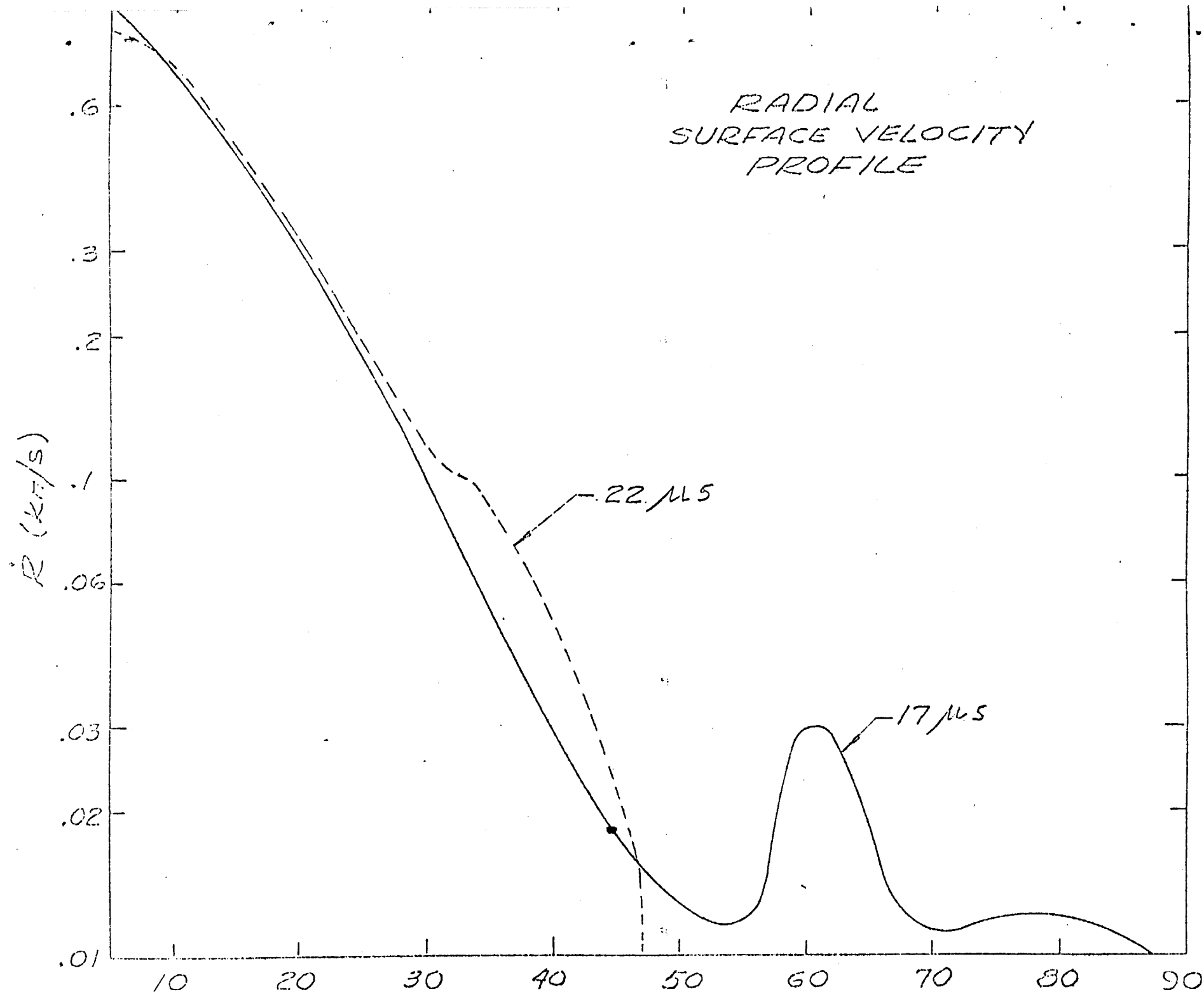SURFACE KINETIC ENERGY
VS
RADIAL DISTANCE

$$f(r) = e^{-3r/D}$$
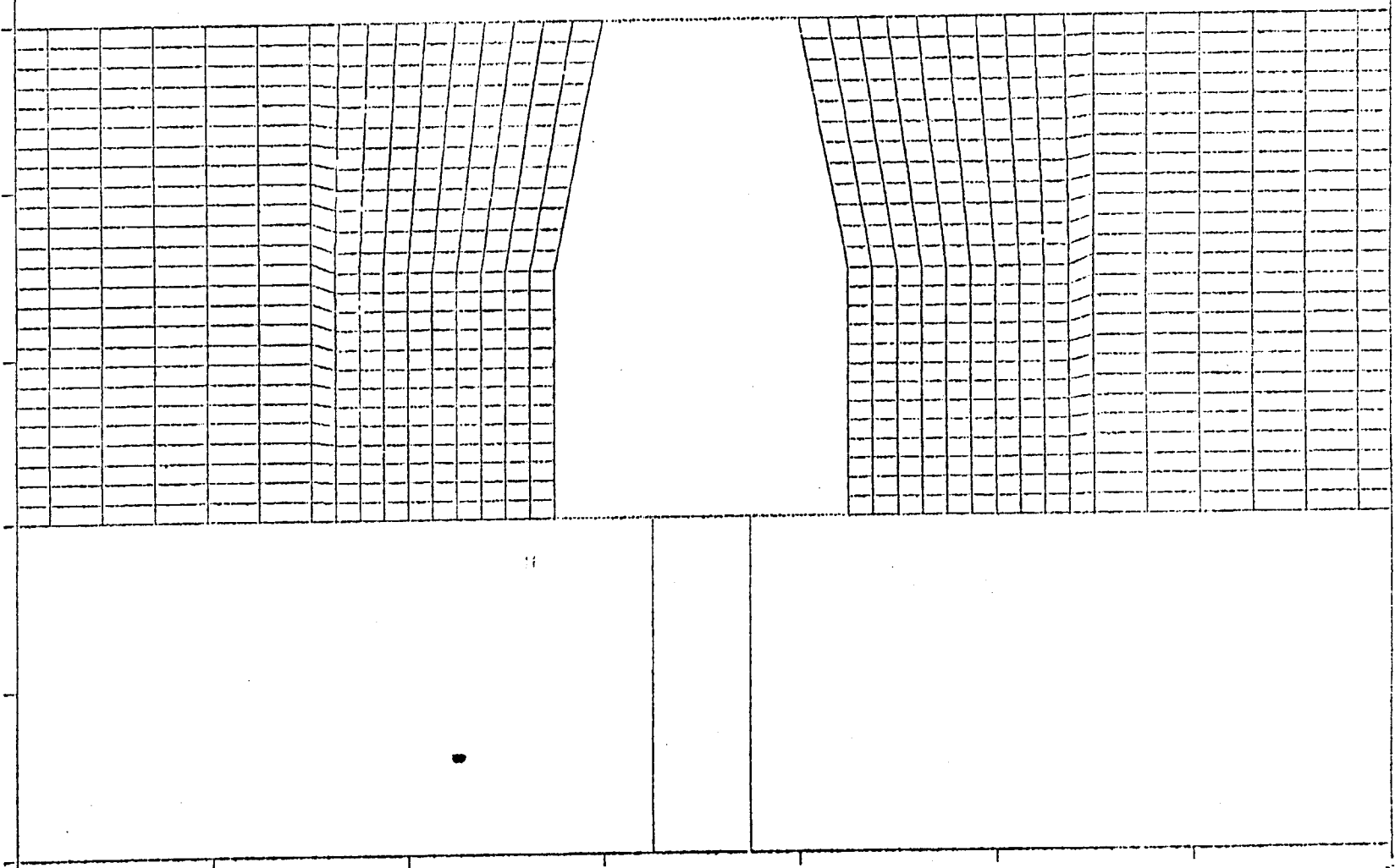
Fig. 5

RADIAL SURFACE VELOCITY PROFILE

Fig. 7